JACS
JOURNAL OF THE AMERICAN CHEMICAL SOCIETY
pubs.acs.org/JACS
Article

Visible-Light-Enabled *Ortho*-Selective Aminopyridylation of Alkenes with *N*-Aminopyridinium Ylides

Yonghoon Moon, Wooseok Lee, and Sungwoo Hong*

Cite This: https://dx.doi.org/10.1021/jacs.0c05025
Read Online

ABSTRACT: By utilizing an underexplored reactivity mode of *N*-aminopyridinium ylides, we developed the visible-light-induced *ortho*-selective aminopyridylation of alkenes via radical-mediated 1,3-dipolar cycloaddition. The photocatalyzed single-electron oxidation of *N*-aminopyridinium ylides generates the corresponding radical cations that enable previously inaccessible 1,3-cycloaddition with a broader range of alkene substrates. The resulting cycloaddition adducts rapidly undergo subsequent homolytic cleavage of the N−N bond, conferring a substantial thermodynamic driving force to yield various *β*-aminoethylpyridines. Remarkably, amino and pyridyl groups can be installed into both activated and unactivated alkenes with modular control of *ortho*-selectivity and 1,2-*syn*-diastereoselectivity under metal-free and mild conditions. Combined experimental and computational studies are conducted to clarify the detailed reaction mechanism and the origins of site selectivity and diastereoselectivity.

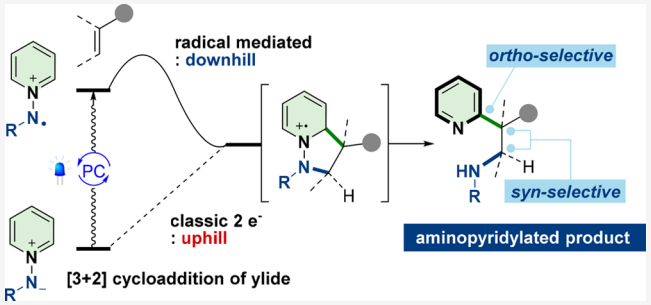

INTRODUCTION

Alkene carboamination that rapidly constructs vicinal C−N and C−C bonds across an alkene is a highly efficient and powerful approach to direct access to structurally diverse *N*-containing molecules in a single operation.[1,2] The *β*-aminoethylpyridine motifs consisting of vicinal pyridine and amino groups are widely employed as versatile building blocks in drug discovery[3] and materials science.[4] In this regard, site-selective and diastereoselective alkene aminopyridylation represents an efficient and robust protocol for installing two valuable pyridine and amino groups onto a carbon−carbon double bond. Despite significant advances, Minisci-type cross-coupling reactions between alkyl radicals and pyridine scaffolds are plagued by poor regioselectivity and overalkylation issues, which precludes the direct use of unblocked pyridine systems.[5]

The synthetic potential of pyridinium salts has been demonstrated as versatile pyridine surrogates to address various chemical transformations.[6] In light of these benefits, our group leveraged the steric and electronic properties of the *N*-substituent of pyridinium salts to control the functionalization of pyridine at the C4-position over the competing C2-position (Scheme 1a).[7] However, the selective introduction of alkyl groups at the C2-position of unblocked pyridinium salts proved uniquely challenging.[8] Driven by the need for an efficient synthetic route to C2-pyridyl *β*-amino motifs, we sought to develop a general strategy that enables the intermolecular *ortho*-selective aminopyridylation of various olefins.

The 1,3-dipolar cycloadditions across C−C *π*-systems are widely employed in the construction of various heterocycles controlling regioselectivity and diastereoselectivity.[9] Despite being less reactive nucleophiles, the *N*-aminopyridinium ylides are capable of undergoing thermally induced 1,3-dipolar cycloadditions with alkynes.[10] Inspired by this strategy, we imagined that the challenging *ortho*-selective aminopyridylation of alkenes could be achieved by exploiting the intermolecular 1,3-dipolar cycloaddition of *N*-aminopyridinium ylides with alkenes. We speculated that the resulting cycloaddition adducts could be converted into the desired C2-pyridyl *β*-amino compounds by subsequent reductive cleavage of the N−N bond of the resulting adducts (Scheme 1b).[7c] In contrast to cycloaddition reactions with alkynes, however, the reaction of *N*-aminopyridinium ylides with olefins has proven to be challenging in classic two-electron chemistry and, to the best of our knowledge, is unprecedented. To understand the curious difference between alkenes and alkynes in behavior toward 1,3-dipolar cycloaddition with *N*-aminopyridinium ylides, we calculated the Gibbs free energies of five-membered cyclized adducts, as shown in Figure 1. These initial computational studies clearly revealed that the impediments to this type of cycloaddition can be attributed to the high-energy barrier of the resulting adducts. Although the

Received: May 7, 2020

Scheme 1. Design Plan: Photocatalytic *ortho*-Selective Aminopyridylation of Olefins Using *N*-Aminopyridinium Ylides

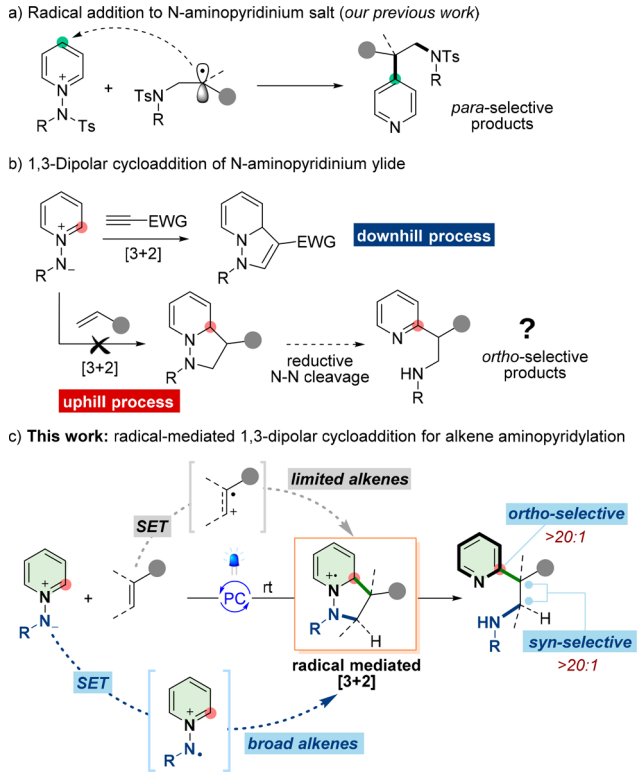

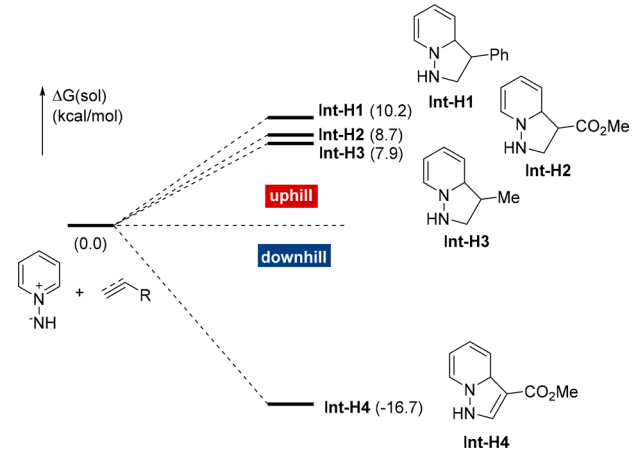

Figure 1. Free energy comparison between *N*-aminopyridinium ylide and their classic [3 + 2] cycloadded product with various alkenes and an alkyne.

cycloaddition reaction with an alkyne was observed to be a thermodynamically downhill process (**Int-H4**, −16.7 kcal/mol), the corresponding reactions with various alkenes were considerably endergonic (**Int-H1**, **H2**, and **H3**, from 7.9 to 10.2 kcal/mol). These observations indicate that the formation of cycloaddition adducts from alkenes is a thermodynamically uphill process and lacks a driving force, thus favoring a competitive retro-1,3-dipolar cycloaddition process (Figure 1). In this regard, an alternative nonclassical strategy is apparently required to overcome the thermodynamic barrier of classic 1,3-dipolar cycloaddition.

We reasoned that the use of open-shell radical cation species from either an *N*-aminopyridinium ylide or alkene would provide an energetic driving force and enable a stepwise 1,3-dipolar cycloaddition. To explore such a strategy, we considered two different approaches to radical-mediated 1,3-dipolar cycloaddition: (1) single-electron-transfer (SET) oxidation of alkenes to generate electrophilic alkene radical cations[11,12] that react with nucleophilic *N*-aminopyridinium ylides and (2) photocatalytic generation of *N*-radical pyridinium salts to enable radical addition to the C−C π-systems of alkenes. The strategy of the photocatalytic alkene carboamination through alkene radical cation intermediates has provided efficient synthetic access to structurally diverse amine derivatives.[12,13] Although remarkable advances have been realized, this approach restricts the alkene scope because the oxidation potentials of some common unactivated alkenes (i.e., terminal aliphatic olefins) prohibitively exceed the redox potentials of even highly oxidizing excited-state photocatalysts as illustrated in Figure 2.[14] As such, this approach is currently limited to the carboamination reactions of activated alkenes, such as styrene analogues and trisubstituted alkyl alkenes.

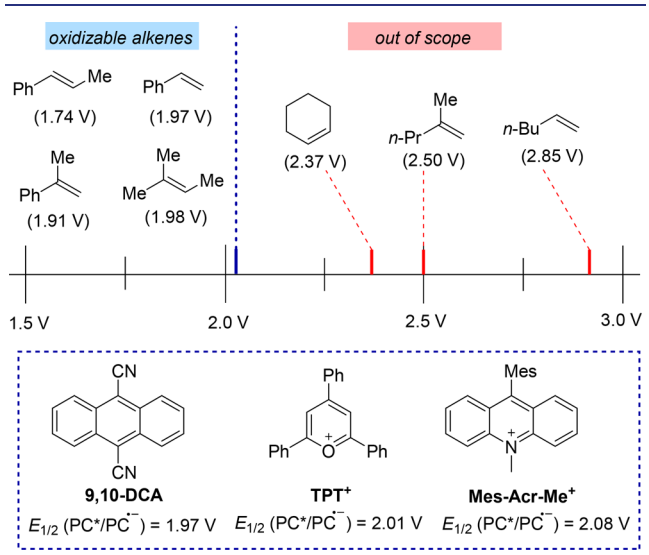

Figure 2. Comparison of redox potentials between highly oxidizing photocatalysts and typical alkenes (vs SCE).

The Knowles group reported the photocatalytic hydroamination reactions of unactivated olefins using nitrogen-centered radicals generated via single-electron-transfer oxidation.[15] With the goal of *ortho*-selective aminopyridylation of various olefins, we envisioned that the direct oxidation of *N*-aminopyridinium ylides by an excited-state redox photocatalyst[16] could generate *N*-radicals that enable previously inaccessible 1,3-cycloaddition with a broader range of alkene substrates, including terminal aliphatic alkenes in the reaction scope. In our working hypothesis, the resulting cycloaddition adducts would undergo subsequent homolytic cleavage of the N−N bond, conferring a substantial thermodynamic driving force to afford the aminopyridylated products, as outlined in Scheme 1c. Herein, we report the successful realization of the *ortho*-selective aminopyridylation of alkenes via previously underexplored photocatalytic radical-mediated 1,3-dipolar cycloaddition using a novel reactivity of *N*-aminopyridinium ylides as bifunctional reagents.[13,17] Remarkably, amino and pyridyl groups could be installed into both activated and

https://dx.doi.org/10.1021/jacs.0c05025
J. Am. Chem. Soc. XXXX, XXX, XXX−XXX

unactivated alkenes with excellent diastereocontrol under metal-free and mild reaction conditions, granting efficient access to a variety of valuable C2-pyridyl β-amino molecules with a *syn*-configuration.

RESULTS AND DISCUSSION

To evaluate the feasibility of using *N*-aminopyridinium ylides for the prospective radical-mediated 1,3-cycloaddition, the model reactions of *N*-aminopyridinium ylide **1** and styrene (**2a**) were conducted in the presence of a photocatalyst under irradiation with blue LEDs (Table 1). Attempts to use *N*-aminopyridinium ylide **1a** failed to produce any product (entry 1). Thus, the success of the proposed strategy requires a suitable *N*-aminopyridinium ylide that can readily undergo single-electron oxidation under mild reaction conditions.

Table 1. Optimization of the Reaction Conditions[a]

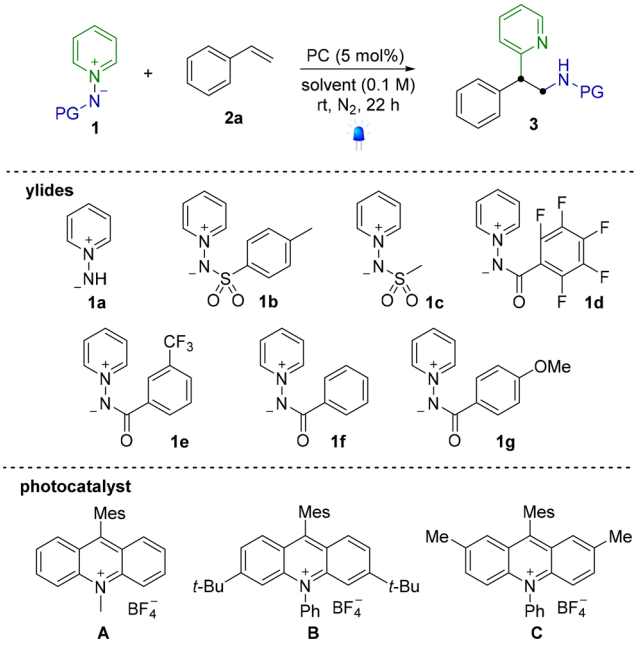

entry	ylide	photocatalyst (5 mol %)	solvent	yield[b] (%)
1	**1a**[c]	**A**	1,2-DCE	n.d.
2	**1b**	**A**	1,2-DCE	13
3	**1c**	**A**	1,2-DCE	13
4	**1d**	**A**	1,2-DCE	n.d.
5	**1e**	**A**	1,2-DCE	19
6	**1f**	**A**	1,2-DCE	37
7	**1g**	**A**	1,2-DCE	59
8	**1g**	**B**	1,2-DCE	69
9	**1g**	**C**	1,2-DCE	71
10	**1g**	**C**	DCM	78
11	**1g**	**C**	MeCN	51
12	**1g**		DCM	n.d.
13[d]	**1g**	**C**	DCM	n.d.
14[e]	**1g**	**C**	DCM	n.d.

[a]Reaction conditions: Ylides (0.1 mmol), **2a** (0.1 mmol), and photocatalyst (5.0 mol %) in solvent (1.0 mL) under irradiation using blue LEDs at rt for 22 h under N_2. [b]Yields were determined by ^{1}H NMR spectroscopy. [c]**1a** was generated from *N*-aminopyridinium iodide and K_2CO_3. [d]Reaction was performed in the dark. [e]TEMPO (1.0 equiv) was added. 1,2-DCE = 1,2-dichloroethane. DCM = dichloromethane, n.d. = not detected.

Because *N*-aminopyridinium salts with different *N*-protecting groups could exhibit distinctive chemical and physical properties, our initial investigations focused on extensive screening of a variety of *N*-aminopyridinium ylides to determine the effect of the *N*-substituent unit on the oxidizable ability of each pyridinium ylide (see the Supporting Information for further details). To our delight, we found that the desired aminopyridylated product **3** could be formed in an *ortho*-selective manner when the sulfonamide group was used as an *N*-substituent (entries 2 and 3). With this promising result in hand, we investigated a series of amide-substituted pyridinium ylides by varying the electron density (entries 4–7). Whereas electron-deficient benzoyl groups showed poor yields (entries 4 and 5), the electron-rich *para*-methoxybenzoyl group **1g** was found to be a superior *N*-substituent to promote aminopyridylation, consistent with its higher oxidizable ability (entry 7). Thus, ylide **1g** was selected for further study. The employment of **C** as a photocatalyst was found to be more productive (entry 9). The evaluation of the solvent revealed that this transformation proceeds best in dichloromethane and produces the product **3a** in 78% yield (entries 10 and 11). We conducted control experiments to confirm the essential role of light and photocatalyst in the success of this transformation (entries 12 and 13). As expected, the desired product was not observed with the recovery of the starting materials when the reaction was conducted with 2,2,6,6-tetramethylpiperidine-1-oxyl (TEMPO) (entry 14).

With the optimized conditions in hand, we set out to examine the substrate scope to verify the generality of the current aminopyridylation reaction, as shown in Table 2. Regarding the alkene scope, this method was applicable to a variety of styrene derivatives, unactivated alkenes, and electron-rich alkenes and allowed excellent functional group tolerance. Styrenes bearing various C4 substituents, including halides (**3b–3d**), bulky *tert*-butyl (**3e**), methoxy (**3f**), trifluoromethyl (**3g**), and trimethylsilyl (**3h**) groups reacted well to form β-aminopyridine derivatives with excellent *ortho*-regiocontrol on the pyridyl scaffold. The *meta*- or *ortho*-substituted (**3j** and **3k**) styrenes showed similar reactivity with *para*-substituted styrene (**3i**). Mesityl styrene and naphthylstyrene were also suitable substrates (**3l** and **3m**). Moreover, various β-aminoethylpyridines containing quaternary carbon centers were readily prepared (**3n–3r**). Typically, the alkene carboamination of unactivated alkenes has proven difficult to achieve through the single-electron oxidation of alkenes. Remarkably, this strategy was not limited to styrene analogues but could also be successfully extended to more challenging substrates, such as terminal aliphatic alkenes (**3s–3y**), highlighting the advantage of the current method involving *N*-centered radical-mediated alkene functionalization. In addition, the scope could be expanded to the electron-rich enol ether and vinyl lactam to afford the desired product **3z** and **3aa**, respectively.

Following the investigations of the alkene scope, we subsequently examined the utility of our method by exploring pyridinium ylide scope. A wide range of pyridinium ylides bearing various functional groups, such as methyl (**4a**), phenyl (**4b**), ketone (**4f**), and substituted aryl groups (methoxy, bromo, and trifluoromethyl) at the C2-position, effectively underwent aminopyridylation to afford the desired products. The resulting 2-phenylpyridine moiety (**4b–4e**) could be widely employed as versatile ligands for designing transition-metal catalysts. For the C2/C3 disubstituted pyridine core, the

https://dx.doi.org/10.1021/jacs.0c05025
J. Am. Chem. Soc. XXXX, XXX, XXX–XXX

Table 2. Substrate Scope of *ortho*-Selective Aminopyridylation[a]

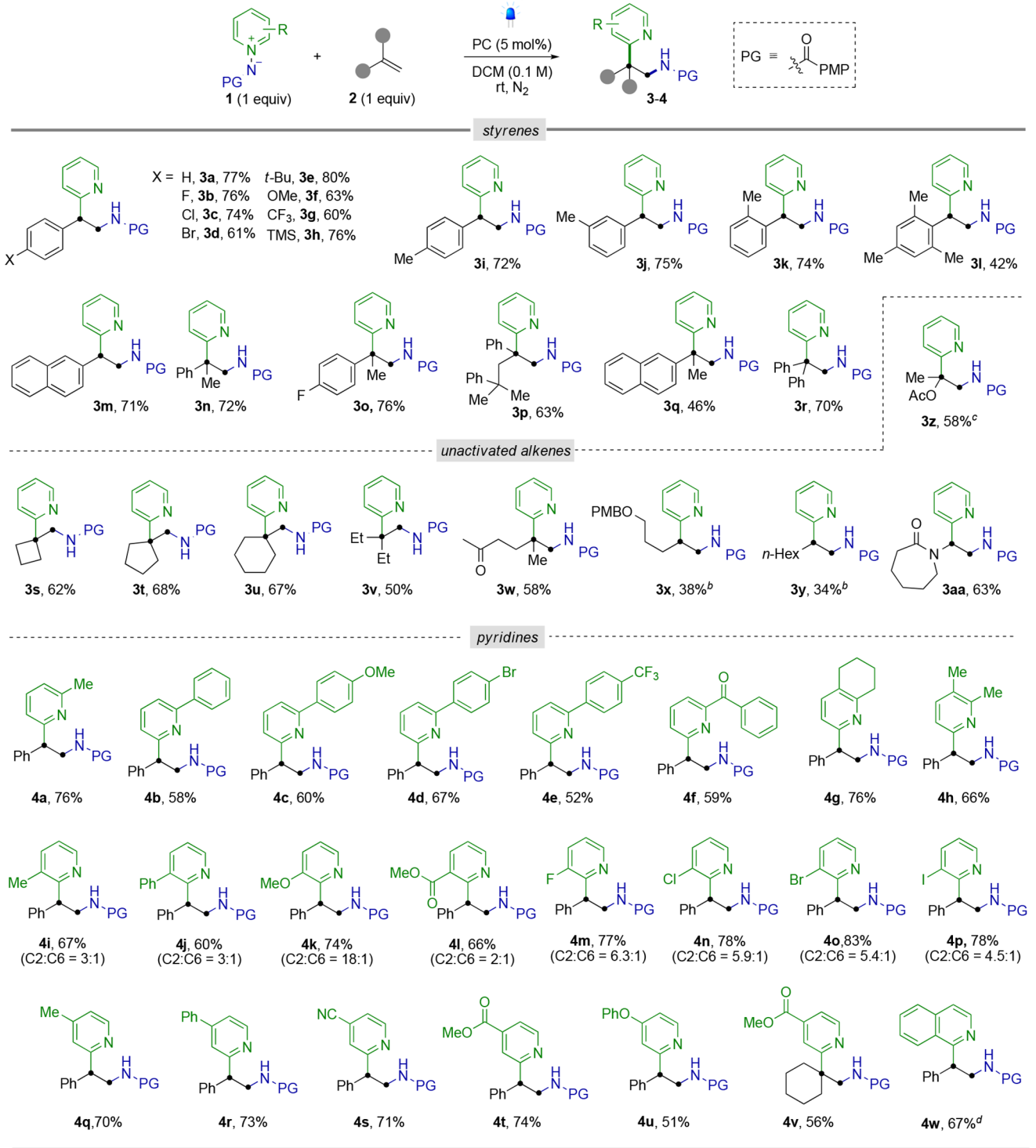

[a]Reaction conditions: **1** (0.1 mmol), **2** (0.1 mmol), and 9-Mes-2,7-di-Me-10-Ph-Acr$^+$BF$_4^-$ (5.0 mol %) in DCM (1.0 mL) under irradiation using blue LEDs at rt for 22 h under N_2. Isolated yields. Regioisomeric ratios were determined by ^{1}H NMR spectroscopy. [b]5.0 equiv of alkene was used. [c]3.0 equiv of alkene was used. [d]Ir[(dFCF$_3$ppy)$_2$(5,5′-dCF$_3$bpy)]PF$_6$ (2.5 mol %) was used as the catalyst.

reactivity was consistent to deliver aminopyridylated products **4g** and **4h**. With respect to the C3-substituted pyridine substrates, radical addition occurred preferably at the sterically more congested C2-position of the pyridine core over the competing C6-position to forge a challenging C−C bond at a sterically more hindered site (**4i**−**4p**). The structure of **4i** was unambiguously confirmed by X-ray analysis of a single crystal (see the Supporting Information for further details). These results could be explained by considering that the initial formation of free radicals on tertiary carbons is likely to be more favorable than the free radicals on secondary carbons as the radical addition converts the sp^2 carbons of the pyridine segment into sp^3 carbons.

https://dx.doi.org/10.1021/jacs.0c05025
J. Am. Chem. Soc. XXXX, XXX, XXX−XXX

Next, C4-substituted pyridinium ylides bearing methyl, phenyl, cyano, ester, and ether were tested with styrene, all showing excellent reactivity (**4q**–**4u**). In addition, aminopyridylation of the unactivated terminal alkene with C4-ester-substituted pyridinium ylide was tolerated under the optimized conditions (**4v**). Further exploration demonstrated that the *N*-isoquinolinium ylide was a suitable substrate and provided the desired product **4w**.

We then attempted to evaluate the scope of internal alkenes, as shown in Table 3. We were pleased to find that this protocol

Table 3. Substrate Scope of Internal Alkenes[a]

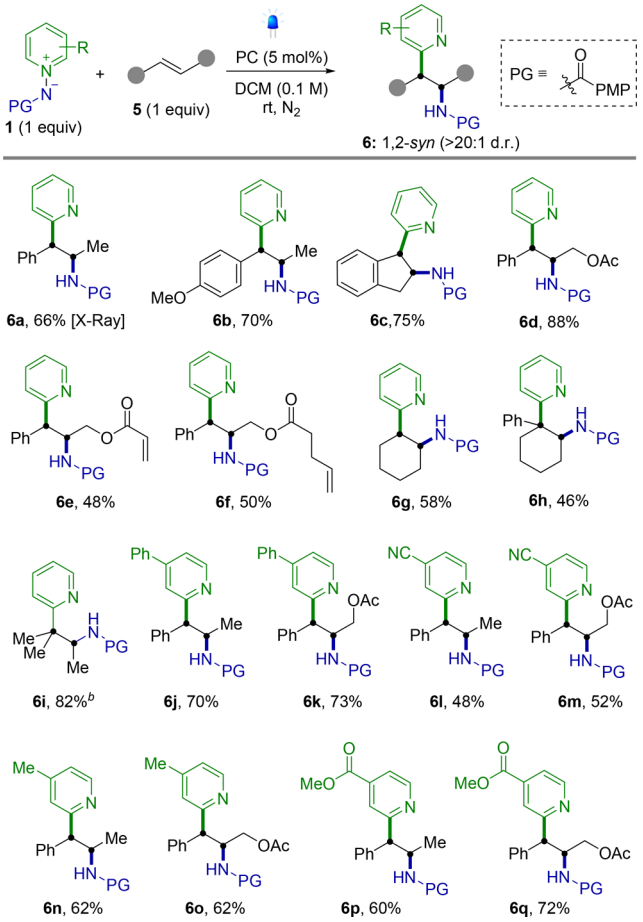

[a]Reaction conditions: **1** (0.1 mmol), **5** (0.1 mmol), and 9-Mes-2,7-di-Me-10-Ph-Acr$^+$BF$_4^-$ (5.0 mol %) in DCM (1.0 mL) under irradiation using blue LEDs at rt for 22 h under N_2. Isolated yields. [b]3.0 equiv of **5i** was used.

was amenable to a range of internal olefins, leading to the formation of 1,2-*syn*-isomeric products with excellent diastereoselectivity (>20:1 d.r.) in all of these examples. The *syn*-configuration between the pyridine and amide groups was unambiguously confirmed by X-ray analysis of a single crystal (**6a**, see the Supporting Information for further details). The applicability of the protocol of indene and cinnamyl acetate was also examined, which led to the formation of desired products **6c** and **6d**. For internal styrenes containing a Michael acceptor or terminal olefin, high chemoselectivity for the styryl double bond was observed (**6e** and **6f**). Substrates bearing cyclohexene were also tolerable to form *syn*-product **6g** and **6h**. Aliphatic trisubstituted alkene underwent aminopyridylation to give **6i** in good yield and regioselectivity. Next, we examined various pyridinium ylides with internal olefins to demonstrate the generality of the diastereoselectivity (**6j**–**6q**). As such, the current method provides an opportunity for accessing 1,2-*syn*-aminopyridylation products.

To further demonstrate the synthetic utility of the current transformation, we explored the late-stage modifications of more structurally complex biorelevant molecules, as highlighted in Table 4. The isoeugenol derivative and *β*-pinene

Table 4. Late-Stage Site-Selective Functionalization of Biorelevant Molecules[a]

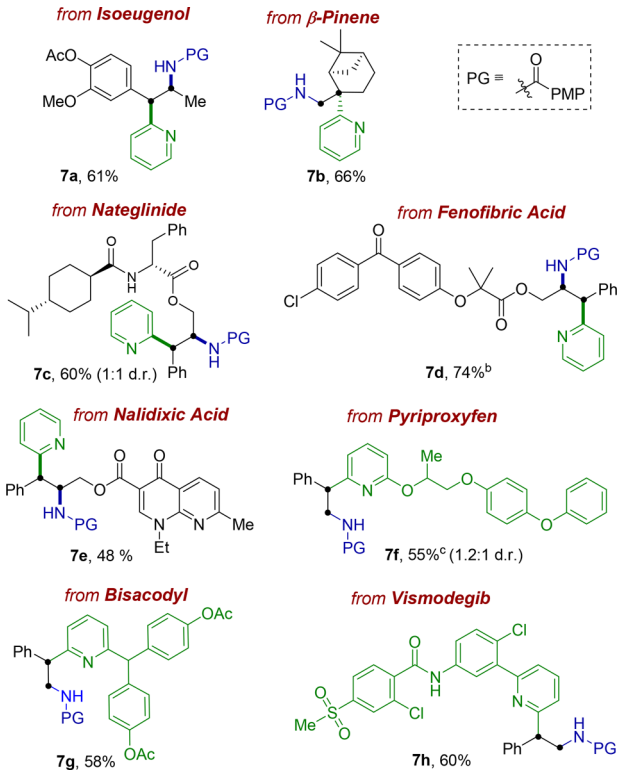

[a]Reaction conditions: **1** (0.1 mmol), alkene (0.1 mmol), and 9-Mes-2,7-di-Me-10-Ph-Acr$^+$BF$_4^-$ (5.0 mol %) in DCM (1.0 mL) under irradiation using blue LEDs at rt for 22 h under N_2. Isolated yields. Regioisomeric ratios were were determined by ^{1}H NMR spectroscopy. [b]2 equiv of **1g** was used. [c]Ir[(dFCF$_3$ ppy)$_2$(5,5′-dCF$_3$ bpy)]PF$_6$ (2.5 mol %), 3 equiv of **2a** was used.

were subjected to the standard reaction conditions, leading to the respective products **7a** and **7b**. Likewise, nateglinide, fenofibric acid, and nalidixic acid derivatives were well-tolerated, affording aminoethylpyridine products **7c**, **7d**, and **7e**. Moreover, substrates derived from pyridine-based drugs with various functional groups, such as pyriproxyfen, bisacodyl, and vismodegib, could be applied to successfully deliver products **7f**, **7g**, and **7h**, respectively. Taken together, these results highlight the synthetic utility of this transformation for rapidly accessing a wide range of valuable C2-aminoalkyl-functionalized pyridine motifs with excellent functional group tolerance, such as ester, ketone, amide, sulfone, ether, and pyridyl groups.

To gain deeper insights into the reaction mechanism and the diastereo-determining step, we carried out computational studies based on density functional theory (DFT). The computed reaction energy profiles are depicted in Figure 3 (see the Supporting Information for details). The reaction is

https://dx.doi.org/10.1021/jacs.0c05025
J. Am. Chem. Soc. XXXX, XXX, XXX−XXX

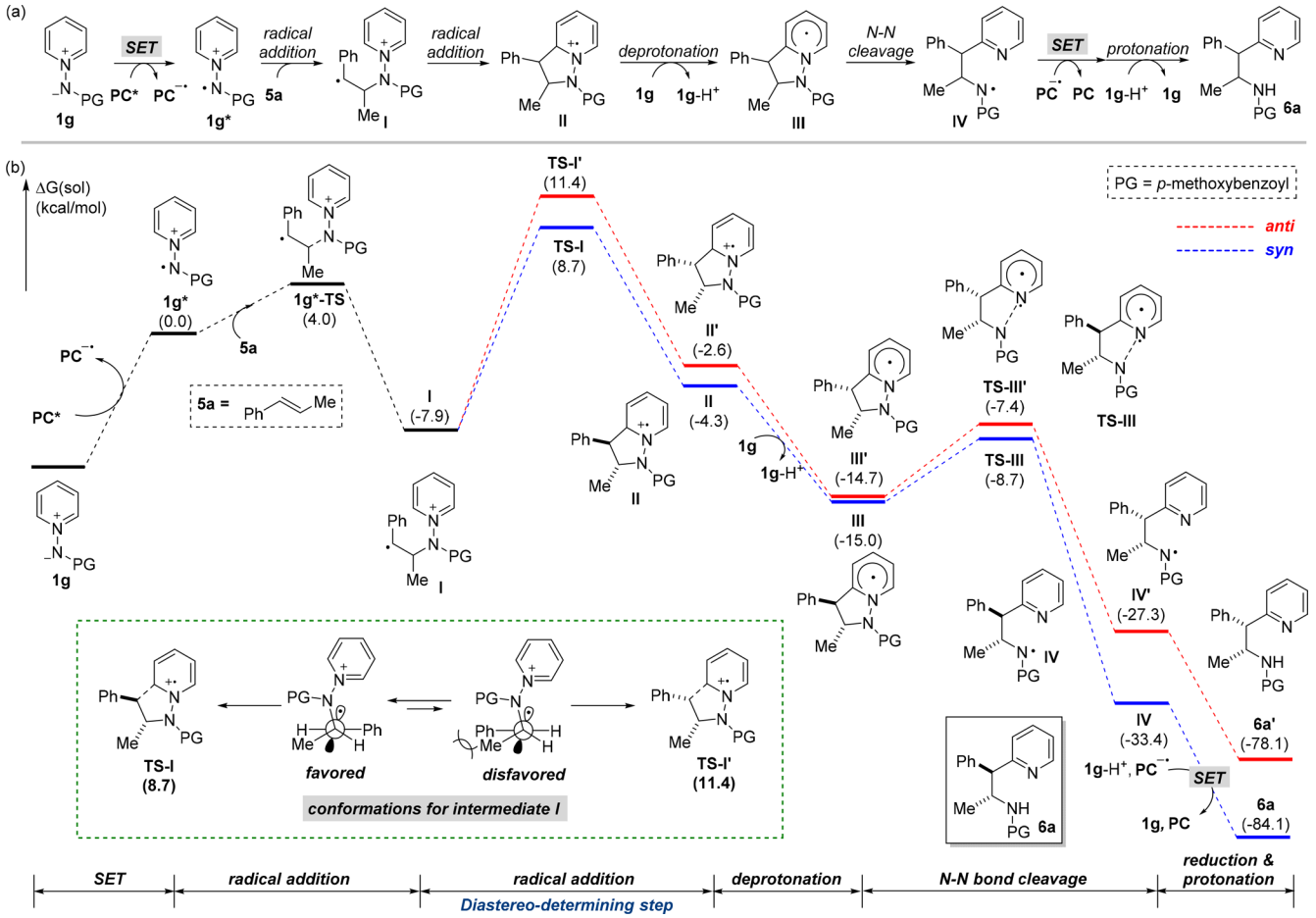

Figure 3. Proposed reaction pathway and related free energy profile. Geometry, vibrational frequency, and solvation energy were calculated using the B3LYP-D3 and LACVP**, and B3LYP-D3 and cc-pVTZ(-f) were employed to determine single-point energy.

initiated by the photoexcitation of PC to the excited state PC*, which oxidizes **1g** to **1g*** via a SET event. The resulting pyridinium radical cation **1g*** reacts with alkene **5a** via **1g*-TS** with a barrier of 4.0 kcal/mol, generating alkyl radical intermediate **I**. Once radical **I** is formed, it is poised for intramolecular radical addition to the C2-position of the pyridinium segment. Our calculations indicate that this radical addition step via **TS-I** determines the diastereoselectivity, leading to the formation of two possible cycloaddition adducts **II** and **II′**. The transition-state **TS-I** that leads to the *syn*-isomer **3n** is 2.7 kcal/mol lower than **TS-I′**. This finding is in good agreement with the experimentally observed excellent diastereoselectivity. Next, the resulting intermediate **II** undergoes deprotonation to form intermediate **III**, and N−N cleavage of intermediate **III** through **TS-III** is fast and energetically downhill (18.4 kcal/mol).

We conducted a kinetic isotope effect (KIE) experiment with **1g** and d5-**1g** as substrates, in which the K_H/K_D ratio was found to be 1.01 (see Scheme 2a), indicating that the deprotonation step is not involved in a rate-determining step in a significant way. Next, *N*-centered radical **IV** is reduced by the PC radical anion, which completes the photocatalytic cycle. Subsequent protonation generates the desired product **6a**. Once the radical intermediate **1g*** is generated, the reaction is highly exergonic, making the overall reaction exothermic by 84.1 kcal/mol, and the intramolecular radical addition is assigned as a diastereo-determining step based on the reaction energy profile. The energy calculation of **6a** and **6a′** indicated that the *syn*-isomer **6a** is a kinetically and thermodynamically more favorable isomer. The reaction quantum yield was found to be Φ = 0.141 (see the Supporting Information for further details), which indicates that a radical chain pathway is not the major pathway in this transformation.

Next, Stern−Volmer quenching studies were conducted, which revealed that the excited state of photocatalyst **C** can be quenched and linearly correlated with the concentration by both pyridinium ylide **1g** and styrene **2a** (Figure 4). However, the Stern−Volmer quenching constant, K_{sv}, of **1g** is significantly higher (>19 times) than that of styrene **2a**. Moreover, a series of Stern−Volmer experiments showed that the luminescence of the photoexcited **C** is barely quenched by unactivated alkenes **2u** and **5g** that were successfully employed in this transformation. In addition, the measured reduction potential of pyridinium ylide **1g** was 1.58 V (peak potential vs SCE, see Figure S7), which is much lower than the reduction potential of styrene (1.97 V vs SCE) and the excited-state catalyst **C** (2.09 V vs SCE). These observations suggested that pyridinium ylides are more favorable for oxidation in the reductive quenching photocatalytic cycle, and therefore the photocatalytic cycle could be reasonably postulated to commence with single-electron oxidation of *N*-aminopyridinium ylides.

To scrutinize the proposed mechanism, several control experiments were conducted. First, the KIE was not observed,

https://dx.doi.org/10.1021/jacs.0c05025
J. Am. Chem. Soc. XXXX, XXX, XXX−XXX

Scheme 2. Control Experiments

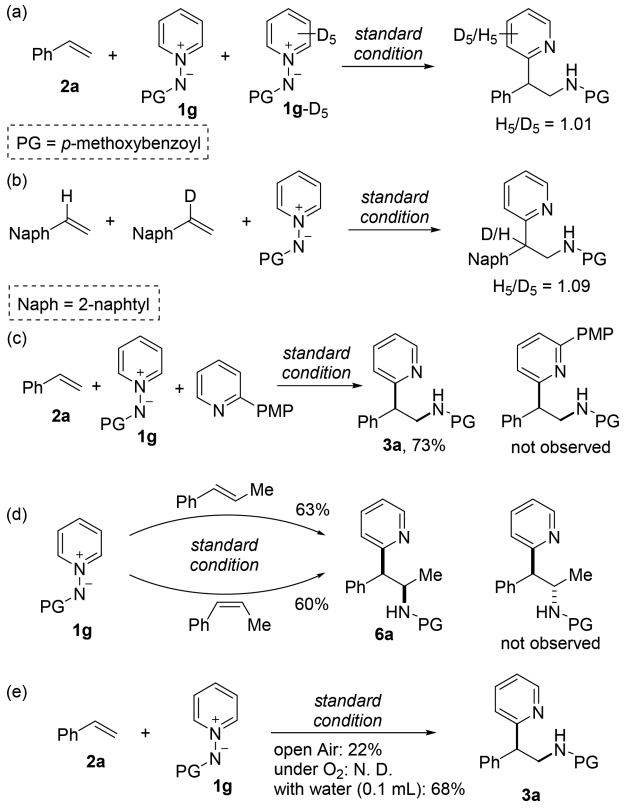

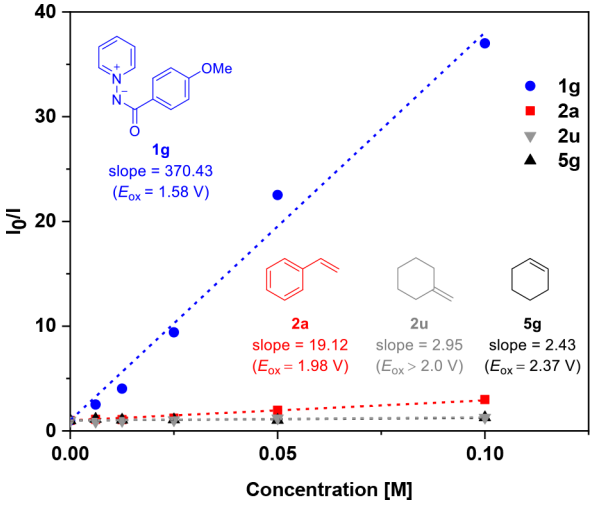

Figure 4. Stern–Volmer quenching plots of photocatalyst **C** with **1g**, **2a**, **2u**, and **5g**.

which indicates that the deprotonation step and intramolecular radical addition step are unlikely to be rate-determining (Scheme 2a,b). To determine whether the pyridine in situ generated from pyridinium ylide via single-electron reduction could act as an alkyl radical acceptor, we subjected mixtures of **1g** and PMP-substituted pyridine to the standard reaction conditions (Scheme 2c), which showed that the functionalization took place only at the pyridinium ylide **1g**. Notably, the reactions with both *Z*- and *E*-methylstyrenes provided the same *syn*-isomeric product **6a**, suggesting that the bond rotation of intermediate **I** is operative in the proposed stepwise cycloaddition process (Scheme 2d and Figure 3). Next, the sensitivity of this method was investigated to determine the influence of the variation of the standard conditions (Scheme 2e). Specifically, the transformation was shown to be insensitive toward moisture. In contrast, the reaction was markedly inhibited under a high-oxygen atmosphere.

CONCLUSIONS

In summary, we have developed a general photocatalytic platform that uses *N*-aminopyridinium ylides as bifunctional reagents to enable *ortho*-selective aminopyridylation of alkenes via radical-mediated 1,3-dipolar cycloaddition with high levels of atom and step economy. Intriguingly, the unprecedented reactivity of the *N*-aminopyridinium radical cations in situ generated from *N*-aminopyridinium ylides via SET has been demonstrated by enabling previously underexplored 1,3-cycloaddition with both activated and unactivated alkenes. The synthetic advances of this transformation allow the functionalization of the pyridine core exclusively at the C2-position. Moreover, the reactions with internal olefins lead to the formation of single diastereomers with a *syn*-configuration. This straightforward and environmentally friendly method exhibited a broad substrate scope at room temperature, and the synthetic value was further demonstrated by late-stage modifications of complex biorelevant molecules. We anticipate that the current method will provide an efficient synthetic toolbox for the modular assembly of valuable *β*-aminoethylpyridines by addressing key challenges of alkene aminopyridylation, including *ortho*-selectivity and diastereoselectivity issues.

ASSOCIATED CONTENT

Supporting Information

The Supporting Information is available free of charge at https://pubs.acs.org/doi/10.1021/jacs.0c05025.

Experimental procedure and characterization of new compounds (^{1}H and ^{13}C NMR spectra) (PDF)

X-ray crystallographic data (**6a**) (CIF)

X-ray crystallographic data (**4i** (major)) (CIF)

X-ray crystallographic data (**4i′** (minor)) (CIF)

AUTHOR INFORMATION

Corresponding Author

Sungwoo Hong − *Department of Chemistry, Korea Advanced Institute of Science and Technology (KAIST), Daejeon 34141, Korea; Center for Catalytic Hydrocarbon Functionalizations, Institute for Basic Science (IBS), Daejeon 34141, Korea;* orcid.org/0000-0001-9371-1730; Email: hongorg@kaist.ac.kr

Authors

Yonghoon Moon − *Department of Chemistry, Korea Advanced Institute of Science and Technology (KAIST), Daejeon 34141, Korea; Center for Catalytic Hydrocarbon Functionalizations, Institute for Basic Science (IBS), Daejeon 34141, Korea*

Wooseok Lee − *Department of Chemistry, Korea Advanced Institute of Science and Technology (KAIST), Daejeon 34141, Korea; Center for Catalytic Hydrocarbon Functionalizations, Institute for Basic Science (IBS), Daejeon 34141, Korea*

Complete contact information is available at: https://pubs.acs.org/10.1021/jacs.0c05025

https://dx.doi.org/10.1021/jacs.0c05025
J. Am. Chem. Soc. XXXX, XXX, XXX−XXX

Notes

The authors declare no competing financial interest.

■ ACKNOWLEDGMENTS

This research was supported financially by the Institute for Basic Science (IBS-R010-A2). We thank Dr. Dongwook Kim (IBS) for XRD analysis.

■ REFERENCES

(1) For selected examples of hydroamination of olefin, see: (a) Muller, T. E.; Hultzsch, K. C.; Yus, M.; Foubelo, F.; Tada, M. Hydroamination: Direct Addition of Amines to Alkenes and Alkynes. *Chem. Rev.* **2008**, *108*, 3795−3892. (b) Huang, L.; Arndt, M.; Gooßen, K.; Heydt, H.; Gooßen, L. J. Late Transition Metal-Catalyzed Hydroamination and Hydroamidation. *Chem. Rev.* **2015**, *115*, 2596−2697. (c) Yang, Y.; Shi, S.-L.; Niu, D.; Liu, P.; Buchwald, S. L. Catalytic Asymmetric Hydroamination of Unactivated Internal Olefins to Aliphatic Amines. *Science* **2015**, *349*, 62−66. (d) Lardy, S. W.; Schmidt, V. A. Intermolecular Radical Mediated Anti-Markovnikov Alkene Hydroamination Using *N*-Hydroxyphthalimide. *J. Am. Chem. Soc.* **2018**, *140*, 12318−12322. (e) Feng, S.; Hao, H.; Liu, P.; Buchwald, S. L. Diastereo- and Enantioselective CuH-Catalyzed Hydroamination of Strained Trisubstituted Alkenes. *ACS Catal.* **2020**, *10*, 282−291. (f) Shen, X.; Chen, X.; Chen, J.; Sun, Y.; Cheng, Z.; Lu, Z. Ligand-Promoted Cobalt-Catalyzed Radical Hydroamination of Alkenes. *Nat. Commun.* **2020**, *11*, 783.

(2) For selected examples of carboamination of olefin, see: (a) Zhang, H.; Pu, W.; Xiong, T.; Li, Y.; Zhou, X.; Sun, K.; Liu, Q.; Zhang, Q. Copper-Catalyzed Intermolecular Aminocyanation and Diamination of Alkenes. *Angew. Chem., Int. Ed.* **2013**, *52*, 2529−2533. (b) Liu, Y.-Y.; Yang, X.-H.; Song, R.-J.; Luo, S.; Li, J.-H. Oxidative 1,2-Carboamination of Alkenes with Alkyl Nitriles and Amines toward Gamma-Amino Alkyl Nitriles. *Nat. Commun.* **2017**, *8*, 14720. (c) Qian, B.; Chen, S.; Wang, T.; Zhang, X.; Bao, H. Iron-Catalyzed Carboamination of Olefins: Synthesis of Amines and Disubstituted *β*-Amino Acids. *J. Am. Chem. Soc.* **2017**, *139*, 13076−13082. (d) Wang, D.; Wang, F.; Chen, P.; Lin, Z.; Liu, G. Enantioselective Copper-Catalyzed Intermolecular Amino- and Azidocyanation of Alkenes in a Radical Process. *Angew. Chem., Int. Ed.* **2017**, *56*, 2054−2058. (e) Wang, D.; Wu, L.; Wang, F.; Wan, X.; Chen, P.; Lin, Z.; Liu, G. Asymmetric Copper-Catalyzed Intermolecular Aminoarylation of Styrenes: Efficient Access to Optical 2,2-Diarylethylamines. *J. Am. Chem. Soc.* **2017**, *139*, 6811−6814. (f) Zhang, Y.; Liu, H.; Tang, L.; Tang, H.-J.; Wang, L.; Zhu, C.; Feng, C. Intermolecular Carboamination of Unactivated Alkenes. *J. Am. Chem. Soc.* **2018**, *140*, 10695−10699. (g) Xiong, H.; Ramkumar, N.; Chiou, M.-F.; Jian, W.; Li, Y.; Su, J.-H.; Zhang, X.; Bao, H. Iron-Catalyzed Carboazidation of Alkenes and Alkynes. *Nat. Commun.* **2019**, *10*, 122. (h) Zheng, S.; Gutiérrez-Bonet, Á.; Molander, G. A. Merging Photoredox PCET with Nickel-Catalyzed Cross-Coupling: Cascade Amidoarylation of Unactivated Olefins. *Chem.* **2019**, *5*, 339−352. (i) He, J.; Xue, Y.; Han, B.; Zhang, C.; Wang, Y.; Zhu, S. Nickel-Catalyzed Asymmetric Reductive 1,2-Carboamination of Unactivated Alkenes. *Angew. Chem., Int. Ed.* **2020**, *59*, 2328−2332. (j) Jiang, H.; Studer, A. Intermolecular Radical Carboamination of Alkenes. *Chem. Soc. Rev.* **2020**, *49*, 1790−1811.

(3) (a) Beavers, M. P.; Myers, M. C.; Shah, P. P.; Purvis, J. E.; Diamond, S. L.; Cooperman, B. S.; Huryn, D. M.; Smith, A. B., III Molecular Docking of Cathepsin L Inhibitors in the Binding Site of Papain. *J. Chem. Inf. Model.* **2008**, *48*, 1464−1472. (b) Kvasnica, M.; Rarova, L.; Oklestkova, J.; Budesinsky, M.; Kohout, L. Synthesis and Cytotoxic Activities of Estrone and Estradiol Cis-Dichloroplatinum-(II) Complexes. *Bioorg. Med. Chem.* **2012**, *20*, 6969−6978.

(4) (a) Dibenedetto, A.; Roth, C. E.; Aresta, M.; Pápai, I. Synthesis and Characterization of Fe(0) (2,2′-Bipyridine) (2-Aminoethyl-Pyridine) and Its Reaction with Dihydrogen. *ChemSusChem* **2017**, *10*, 220−225. (b) Zhang, L.; August, D. P.; Zhong, J.; Whitehead, G. F. S.; Vitorica-Yrezabal, I. J.; Leigh, D. A. Molecular Trefoil Knot from a Trimeric Circular Helicate. *J. Am. Chem. Soc.* **2018**, *140*, 4982−4985.

(5) For selected examples of acid-promoted Minisci reaction, see: (a) O'Hara, F.; Blackmond, D. G.; Baran, P. S. Radical-Based Regioselective C-H Functionalization of Electron-Deficient Heteroarenes: Scope, Tunability, and Predictability. *J. Am. Chem. Soc.* **2013**, *135*, 12122−12134. (b) Jin, J.; MacMillan, D. W. C. Direct *α*-Arylation of Ethers through the Combination of Photoredox-Mediated C-H Functionalization and the Minisci Reaction. *Angew. Chem., Int. Ed.* **2015**, *54*, 1565−1569. (c) Tang, R.-J.; Kang, L.; Yang, L. Metal-Free Oxidative Decarbonylative Coupling of Aliphatic Aldehydes with Azaarenes: Successful Minisci-Type Alkylation of Various Heterocycles. *Adv. Synth. Catal.* **2015**, *357*, 2055−2060. (d) Garza-Sanchez, R. A.; Tlahuext-Aca, A.; Tavakoli, G.; Glorius, F. Visible Light-Mediated Direct Decarboxylative C-H Functionalization of Heteroarenes. *ACS Catal.* **2017**, *7*, 4057−4061. (e) Klauck, F. J. R.; James, M. J.; Glorius, F. Deaminative Strategy for the Visible-Light-Mediated Generation of Alkyl Radicals. *Angew. Chem., Int. Ed.* **2017**, *56*, 12336−12339. (f) Gutiérrez-Bonet, Á.; Remeur, C.; Matsui, J. K.; Molander, G. A. Late-Stage C-H Alkylation of Heterocycles and 1,4-Quinones via Oxidative Homolysis of 1,4-Dihydropyridines. *J. Am. Chem. Soc.* **2017**, *139*, 12251−12258. (g) Wu, X.; Zhang, H.; Tang, N.; Wu, Z.; Wang, D.; Ji, M.; Xu, Y.; Wang, M.; Zhu, C. Metal-Free Alcohol-Directed Regioselective Heteroarylation of Remote Unactivated C(sp^3)-H Bonds. *Nat. Commun.* **2018**, *9*, 3343. (h) Tang, N.; Wu, X.; Zhu, C. Practical, metal-free remote heteroarylation of amides via unactivated C(sp^3-H bond functionalization. *Chem. Sci.* **2019**, *10*, 6915−6919. (i) Li, G.-X.; Hu, X.; He, G.; Chen, G. Photoredox-Mediated Remote C(sp^3)-H Heteroarylation of Free Alcohols. *Chem. Sci.* **2019**, *10*, 688−693. (j) Pitre, S. P.; Muuronen, M.; Fishman, D. A.; Overman, L. E. Tertiary Alcohols as Radical Precursors for the Introduction of Tertiary Substituents into Heteroarenes. *ACS Catal.* **2019**, *9*, 3413−3418.

(6) For selected examples of using pyridinium salt as a radical acceptor, see: (a) Ma, X.; Dang, H.; Rose, J. A.; Rablen, P.; Herzon, S. B. Hydroheteroarylation of Unactivated Alkenes Using *N*-Methoxyheteroarenium Salts. *J. Am. Chem. Soc.* **2017**, *139*, 5998−6007. (b) He, Y.-T.; Kang, D.; Kim, I.; Hong, S. Metal-Free Photocatalytic Trifluoromethylative Pyridylation of Unactivated Alkenes. *Green Chem.* **2018**, *20*, 5209−5214. (c) Kim, I.; Park, B.; Kang, G.; Kim, J.; Jung, H.; Lee, H.; Baik, M.-H.; Hong, S. Visible-Light-Induced Pyridylation of Remote C(sp^3)-H Bonds by Radical Translocation of *N*-Alkoxypyridinium Salts. *Angew. Chem., Int. Ed.* **2018**, *57*, 15517−15522. (d) Kim, I.; Kang, G.; Lee, K.; Park, B.; Kang, D.; Jung, H.; He, Y.-T.; Baik, M.-H.; Hong, S. Site-Selective Functionalization of Pyridinium Derivatives via Visible-Light-Driven Photocatalysis with Quinolinone. *J. Am. Chem. Soc.* **2019**, *141*, 9239−9248. (e) Kim, Y.; Lee, K.; Mathi, G. R.; Kim, I.; Hong, S. Visible-Light-Induced Cascade Radical Ring-Closure and Pyridylation for the Synthesis of Tetrahydrofurans. *Green Chem.* **2019**, *21*, 2082−2087. (f) Jeon, J.; He, Y.-T.; Shin, S.; Hong, S. Visible-Light-Induced *Ortho*-Selective Migration on Pyridyl Ring: Trifluoromethylative Pyridylation of Unactivated Alkenes. *Angew. Chem., Int. Ed.* **2020**, *59*, 281−285. (g) Mathi, G. R.; Jeong, Y.; Moon, Y.; Hong, S. Photochemical Carbopyridylation of Alkenes Using *N*-Alkenoxypyridinium Salts as Bifunctional Reagents. *Angew. Chem., Int. Ed.* **2020**, *59*, 2049−2054. (h) Lee, K.; Lee, S.; Kim, N.; Kim, S.; Hong, S. Visible-Light-Enabled Trifluoromethylative Pyridylation of Alkenes from Pyridines and Triflic Anhydride. *Angew. Chem., Int. Ed.* **2020**, DOI: 10.1002/anie.202004439.

(7) For examples of using *N*-aminopyridinium salt as radical acceptor, see: (a) Jung, S.; Lee, H.; Moon, Y.; Jung, H.-Y.; Hong, S. Site-Selective C-H Acylation of Pyridinium Derivatives by Photoredox Catalysis. *ACS Catal.* **2019**, *9*, 9891−9896. (b) Kim, N.; Lee, C.; Kim, T.; Hong, S. Visible-Light-Induced Remote C(sp^3)-H Pyridylation of Sulfonamides and Carboxamides. *Org. Lett.* **2019**, *21*, 9719−9723. (c) Moon, Y.; Park, B.; Kim, I.; Kang, G.; Shin, S.; Kang, D.; Baik, M.-H.; Hong, S. Visible Light Induced Alkene Aminopyridylation Using

https://dx.doi.org/10.1021/jacs.0c05025
J. Am. Chem. Soc. XXXX, XXX, XXX−XXX

N-Aminopyridinium Salts as Bifunctional Reagents. *Nat. Commun.* **2019**, *10*, 4117.

(8) For selected examples of transition-metal-free alkylation of pyridine *N*-oxides, see: (a) Jo, W.; Kim, J.; Choi, S.; Cho, S. H. Transition-Metal-Free Regioselective Alkylation of Pyridine *N*-Oxides Using 1,1-Diborylalkanes as Alkylating Reagents. *Angew. Chem., Int. Ed.* **2016**, *55*, 9690−9694. (b) Zhou, W.; Miura, T.; Murakami, M. Photocatalyzed *ortho*-Alkylation of Pyridine *N*-Oxides through Alkene Cleavage. *Angew. Chem., Int. Ed.* **2018**, *57*, 5139−5142. (c) Xu, J.-H.; Wu, W.-B.; Wu, J. Photoinduced Divergent Alkylation/Acylation of Pyridine *N*-Oxides with Alkynes under Anaerobic and Aerobic Conditions. *Org. Lett.* **2019**, *21*, 5321−5325.

(9) For selected examples of 1,3-dipolar cycloaddition with ylides, see: (a) Padwa, A.; Austin, D. J.; Precedo, L.; Zhi, L. Cycloaddition Reactions of Pyridinium and Related Azomethine Ylides. *J. Org. Chem.* **1993**, *58*, 1144−1150. (b) Allgäuer, D. S.; Mayer, P.; Mayr, H. Nucleophilicity Parameters of Pyridinium Ylides and Their Use in Mechanistic Analyses. *J. Am. Chem. Soc.* **2013**, *135*, 15216−15224. (c) Hu, R.-B.; Sun, S.; Su, Y. Visible-Light-Induced Carbo-2-Pyridylation of Electron-Deficient Alkenes with Pyridinium Salts. *Angew. Chem., Int. Ed.* **2017**, *56*, 10877−10880.

(10) For selected examples of 1,3-dipolar cycloaddition with *N*-aminopyridinium derivatives, see: (a) Mousseau, J. J.; Bull, J. A.; Ladd, C. L.; Fortier, A.; Sustac Roman, D.; Charette, A. B. Synthesis of 2- and 2,3-Substituted Pyrazolo[1,5-a]Pyridines: Scope and Mechanistic Considerations of a Domino Direct Alkynylation and Cyclization of *N*-Iminopyridinium Ylides Using Alkenyl Bromides, Alkenyl Iodides, and Alkynes. *J. Org. Chem.* **2011**, *76*, 8243−8261. (b) Ding, S.; Yan, Y.; Jiao, N. Copper-Catalyzed Direct Oxidative Annulation of *N*-Iminopyridinium Ylides with Terminal Alkynes Using O_2 as Oxidant. *Chem. Commun.* **2013**, *49*, 4250−4252.

(11) For selected examples of alkene radical cations, see: (a) Ischay, M. A.; Ament, M. S.; Yoon, T. P. Crossed Intermolecular [2 + 2] Cycloaddition of Styrenes by Visible Light Photocatalysis. *Chem. Sci.* **2012**, *3*, 2807−2811. (b) Sarabia, F. J.; Ferreira, E. M. Radical Cation Cyclopropanations via Chromium Photooxidative Catalysis. *Org. Lett.* **2017**, *19*, 2865−2868. (c) Li, Y.; Lu, R.; Sun, S.; Liu, L. Metal-Free Three-Component Oxyalkynylation of Alkenes. *Org. Lett.* **2018**, *20*, 6836−6839. (d) Sarabia, F. J.; Li, Q.; Ferreira, E. M. Cyclopentene Annulations of Alkene Radical Cations with Vinyl Diazo Species Using Photocatalysis. *Angew. Chem., Int. Ed.* **2018**, *57*, 11015−11019. (e) Xiong, P.; Long, H.; Song, J.; Wang, Y.; Li, J.-F.; Xu, H.-C. Electrochemically Enabled Carbohydroxylation of Alkenes with H_2O and Organotrifluoroborates. *J. Am. Chem. Soc.* **2018**, *140*, 16387−16391. (f) Cai, C.-Y.; Shu, X.-M.; Xu, H.-C. Practical and Stereoselective Electrocatalytic 1,2-Diamination of Alkenes. *Nat. Commun.* **2019**, *10*, 4953. (g) Markham, J. P.; Wang, B.; Stevens, E. D.; Burris, S. C.; Deng, Y. *Ortho*-Alkylation of Pyridine *N*-Oxides with Alkynes by Photocatalysis: Pyridine *N*-Oxide as a Redox Auxiliary. *Chem. - Eur. J.* **2019**, *25*, 6638−6644.

(12) For examples of alkene radical cation-mediated reactions published from Nicewicz's group, see: (a) Romero, N. A.; Nicewicz, D. A. Mechanistic Insight into the Photoredox Catalysis of Anti-Markovnikov Alkene Hydrofunctionalization Reactions. *J. Am. Chem. Soc.* **2014**, *136*, 17024−17035. (b) Wilger, D. J.; Grandjean, J.-M.; Lammert, T. R.; Nicewicz, D. A. The Direct Anti-Markovnikov Addition of Mineral Acids to Styrenes. *Nat. Chem.* **2014**, *6*, 720−726. (c) Zeller, M. A.; Riener, M.; Nicewicz, D. A. Butyrolactone Synthesis via Polar Radical Crossover Cycloaddition Reactions: Diastereoselective Syntheses of Methylenolactocin and Protolichesterinic Acid. *Org. Lett.* **2014**, *16*, 4810−4813. (d) Margrey, K. A.; Nicewicz, D. A. A General Approach to Catalytic Alkene Anti-Markovnikov Hydrofunctionalization Reactions via Acridinium Photoredox Catalysis. *Acc. Chem. Res.* **2016**, *49*, 1997−2006. (e) Wu, F.; Wang, L.; Chen, J.; Nicewicz, D. A.; Huang, Y. Direct Synthesis of Polysubstituted Aldehydes via Visible-Light Catalysis. *Angew. Chem., Int. Ed.* **2018**, *57*, 2174−2178. (f) Onuska, N. P. R.; Schutzbach-Horton, M. E.; Rosario Collazo, J. L.; Nicewicz, D. A. Anti-Markovnikov Hydroazidation of Activated Olefins via Organic Photoredox Catalysis. *Synlett* **2020**, *31*, 55−59.

(13) Monos, T. M.; McAtee, R. C.; Stephenson, C. R. J. Arylsulfonylacetamides as Bifunctional Reagents for Alkene Aminoarylation. *Science* **2018**, *361*, 1369−1373.

(14) (a) Roth, H. G.; Romero, N. A.; Nicewicz, D. A. Electrochemical Potentials of Common Organic Molecules for Applications to Single Electron Redox Chemistry. *Synlett* **2016**, *27*, 714−723. (b) Cartwright, K. C.; Tunge, J. A. Decarboxylative Elimination of *N*-Acyl Amino Acids Via Photoredox/Cobalt Dual Catalysis. *ACS Catal.* **2018**, *8*, 11801−11806. (c) Pitre, S. P.; McTiernan, C. D.; Scaiano, J. C. Understanding the Kinetics and Spectroscopy of Photoredox Catalysis and Transition-Metal-Free Alternatives. *Acc. Chem. Res.* **2016**, *49*, 1320−1330.

(15) For selected examples of *N*-centered radical generation and addition to sp^2 carbons, see: (a) Choi, G. J.; Knowles, R. R. Catalytic Alkene Carboaminations Enabled by Oxidative Proton-Coupled Electron Transfer. *J. Am. Chem. Soc.* **2015**, *137*, 9226−9229. (b) Miller, D. C.; Choi, G. J.; Orbe, H. S.; Knowles, R. R. Catalytic Olefin Hydroamidation Enabled by Proton-Coupled Electron Transfer. *J. Am. Chem. Soc.* **2015**, *137*, 13492−13495. (c) Musacchio, A. J.; Lainhart, B. C.; Zhang, X.; Naguib, S. G.; Sherwood, T. C.; Knowles, R. R. Catalytic Intermolecular Hydroaminations of Unactivated Olefins with Secondary Alkyl Amines. *Science* **2017**, *355*, 727−730. (d) Moon, Y.; Jang, E.; Choi, S.; Hong, S. Visible-Light-Photocatalyzed Synthesis of Phenanthridinones and Quinolinones via Direct Oxidative C-H Amidation. *Org. Lett.* **2018**, *20*, 240−243. (e) Zhu, Q.; Graff, D. E.; Knowles, R. R. Intermolecular Anti-Markovnikov Hydroamination of Unactivated Alkenes with Sulfonamides Enabled by Proton-Coupled Electron Transfer. *J. Am. Chem. Soc.* **2018**, *140*, 741−747. (f) Miller, D. C.; Ganley, J. M.; Musacchio, A. J.; Sherwood, T. C.; Ewing, W. R.; Knowles, R. R. Anti-Markovnikov Hydroamination of Unactivated Alkenes with Primary Alkyl Amines. *J. Am. Chem. Soc.* **2019**, *141*, 16590−16594. (g) Nguyen, S. T.; Zhu, Q.; Knowles, R. R. PCET-Enabled Olefin Hydroamidation Reactions with *N*-Alkyl Amides. *ACS Catal.* **2019**, *9*, 4502−4507. (h) Roos, C. B.; Demaerel, J.; Graff, D. E.; Knowles, R. R. Enantioselective Hydroamination of Alkenes with Sulfonamides Enabled by Proton-Coupled Electron Transfer. *J. Am. Chem. Soc.* **2020**, *142*, 5974−5979.

(16) For selected reviews of photoredox catalysis, see: (a) Prier, C. K.; Rankic, D. A.; MacMillan, D. W. C. Visible Light Photoredox Catalysis with Transition Metal Complexes: Applications in Organic Synthesis. *Chem. Rev.* **2013**, *113*, 5322−5363. (b) Romero, N. A.; Nicewicz, D. A. Organic Photoredox Catalysis. *Chem. Rev.* **2016**, *116*, 10075−10166. (c) Shaw, M. H.; Twilton, J.; MacMillan, D. W. C. Photoredox Catalysis in Organic Chemistry. *J. Org. Chem.* **2016**, *81*, 6898−6926. (d) Skubi, K. L.; Blum, T. R.; Yoon, T. P. Dual Catalysis Strategies in Photochemical Synthesis. *Chem. Rev.* **2016**, *116*, 10035−10074. (e) Chatterjee, T.; Iqbal, N.; You, Y.; Cho, E. J. Controlled Fluoroalkylation Reactions by Visible-Light Photoredox Catalysis. *Acc. Chem. Res.* **2016**, *49*, 2284−2294. (f) Wang, C.-S.; Dixneuf, P. H.; Soulé, J.-F. Photoredox Catalysis for Building C-C Bonds from C(sp^2)-H Bonds. *Chem. Rev.* **2018**, *118*, 7532−7585. (g) Zhao, Y.; Xia, W. Recent Advances in Radical-Based C-N Bond Formation Via Photo-/Electrochemistry. *Chem. Soc. Rev.* **2018**, *47*, 2591−2608. (h) Troian-Gautier, L.; Turlington, M. D.; Wehlin, S. A. M.; Maurer, A. B.; Brady, M. D.; Swords, W. B.; Meyer, G. J. Halide Photoredox Chemistry. *Chem. Rev.* **2019**, *119*, 4628−4683. (i) Pagire, S. K.; Föll, T.; Reiser, O. Shining Visible Light on Vinyl Halides: Expanding the Horizons of Photocatalysis. *Acc. Chem. Res.* **2020**, *53*, 782−791. (j) Yu, X.-Y.; Zhao, Q.-Q.; Chen, J.; Xiao, W.-J.; Chen, J.-R. When Light Meets Nitrogen-Centered Radicals: From Reagents to Catalysts. *Acc. Chem. Res.* **2020**, *53*, 1066−1083.

(17) (a) Yu, J.; Wu, Z.; Zhu, C. Efficient Docking-Migration Strategy for Selective Radical Difluoromethylation of Alkenes. *Angew. Chem., Int. Ed.* **2018**, *57*, 17156−17160. (b) Wang, M.; Zhang, H.; Liu, J.; Wu, X.; Zhu, C. Radical Monofluoroalkylative Alkynylation of Olefins by Docking-Migration Strategy. *Angew. Chem.* **2019**, *131* (49),

https://dx.doi.org/10.1021/jacs.0c05025
J. Am. Chem. Soc. XXXX, XXX, XXX−XXX

17810−17814. (c) Liu, J.; Wu, S.; Yu, J.; Lu, C.; Wu, Z.; Wu, X.; Xue, X.-S.; Zhu, C. Polarity Umpolung Strategy for the Radical Alkylation of Alkenes. *Angew. Chem., Int. Ed.* **2020**, *59*, 8195−8202.

https://dx.doi.org/10.1021/jacs.0c05025
J. Am. Chem. Soc. XXXX, XXX, XXX−XXX